Drug Development and Industrial Pharmacy, 33:63–70, 2007

ISSN: 0363-9045 print / 1520-5762 online
DOI: 10.1080/03639040600762636

informa
healthcare

Kinetic Analysis of Chlorpropamide Dissolution from Solid Dispersions

Mohammad Barzegar-Jalali
Department of Pharmaceutics, School of Pharmacy and Drug Applied Research Center, Tabriz University of Medical Sciences, Tabriz, Iran

Siavoush Dastmalchi
Department of Medicinal Chemistry, School of Pharmacy and Biotechnology Research Center, Tabriz University of Medical Sciences, Tabriz, Iran

ABSTRACT Solid dispersions (SDs) of chlorpropamide were prepared by the solvent deposition technique using two grades of microcrystalline cellulose as carrier materials with different ratios of drug to carrier. The dissolution rate of chlorpropmide from the SDs was carried out at two physiological pH values of 1.1 and 7.25 simulating gastric and intestinal environments. The dissolution was dependent on the grade, the ratio of drug to carrier and pH. The higher dissolution was observed for more hydrophilic grade of the carrier as well as the higher ratio of carrier to drug. At the higher pH the drug dissolved much faster than the lower pH. X-ray diffraction showed some reduced drug crystallinity in SDs whereas infrared spectroscopy revealed no drug interactions with solvent and the carriers. The enhanced dissolution was attributed to the reduced drug crystallinity, decreased particle size, increased wettability and reduced aggregation of the hydrophobic drug particles. A novel model denoted as reciprocal powered time model with its theoretical justification was employed to analyze the dissolution data and proved to be superior to commonly used models for the analysis of the data. There was a quantitative relation between the model parameter and the ratio of carrier to drug which could be of value in dissolution rate prediction.

KEYWORDS Chlorpropamide, Solvent deposition, Solid dispersion, Dissolution kinetics, Reciprocal powered time model

INTRODUCTION

Chlorpropamide is a sulfonylurea antidiabetic drug which is given per orally in the treatment of type two diabetes mellitus (Sweetman, 2005). The drug is practically insoluble in water (Sweetman, 2005) that can lead to a poor dissolution which in turn may cause a decrease in the rate of bioavailability. In fact it has been shown that the drug has been absorbed with different rates from various dosage forms (Evans et al., 1979; Batenhorst et al., 1982). Some attempts have been made to increase dissolution rate of chlorpropamide via solid dispersion (SD) technology. Among the various technologies, fusion, and coprecipitation methods involving water soluble carriers have been employed to increase chlorpropamide dissolution (Ford & Rubinstein, 1977; Deshpande & Agrawal, 1983, 1984; Dubois & Ford, 1985). These techniques

Address correspondence to Mohammad Barzegar-Jalali, Department of Pharmaceutics, School of Pharmacy, Tabriz University of Medical Sciences, Tabriz 51664, Iran; Fax: +98 (411) 334 4798; E-mail: barzegar_jalali@yahoo.com

have resulted in increased drug bioavailability and absorption (Deshpande & Agrawal, 1984, 1985). To the best of our knowledge the dissolution of chlorpropamide from SDs prepared by solvent deposition technique involving water insoluble carriers has not been reported previously. In the present work we used two grades of microcrystalline cellulose in various ratios of the drug to the water insoluble carriers to enhance its dissolution at two different physiological pH values of 1.1 and 7.25 simulating gastric and intestinal environments. X-ray diffraction and infrared (IR) spectroscopy methods were advocated to elucidate possible crystal changes in the SDs and drug-carrier as well as solvent interactions. A novel kinetic model denoted as reciprocal powered time model was used to analyze the drug dissolution data and the accuracy of the proposed model was compared with that of available models (Wagner, 1969; Costa & Sousa Lobo, 2001). A theoretical justification for the proposed model has also been provided using the classic Noyes-Whitney dissolution equation (Noyes & Whitney, 1897).

MATERIALS AND METHODS

Materials

Chlorpropamide (Mehta, Mumbai, India), microcrystalline cellulose (either Avicel PH-102 or Avicel RC-591, FMC, Brussels, Belgium), methylene chloride (Merck, Darmstadt, Germany) were used as received. All other materials were analytical grades.

Preparation of SD Systems and Physical mixture

The solvent deposition systems was formulated by dissolving chlorpropamide in methylene chloride to produce a clear solution (Van der watt et al., 1996; Yen et al., 1997; Barzegar-Jalali et al., 2002). The carrier was dispersed in the solution by stirring and the solvent was evaporated at 37 ± 0.5°C. The resultant mass was dried for 24 hr at 40°C, pulverized and passed through a sieve with mesh number of 120. The ratios of drug to carrier were 1:1, 1:2, and 1:5 in the SD systems for both grades of microcrystalline cellulose. A physical mixture containing one part of the drug and five parts of Avicel PH-102 was prepared using the bottle method. Details of the formulations are given in Table 1. Three samples containing 20 mg chlorpropamide were taken from the SDs as well as the physical mixture, dissolved in appropriate volume of phosphate buffer pH 7.25, an aliquot withdrawn, acidified with 1 M HCl and analyzed by UV spectroscopy at a wavelength of 232.6 nm (UV-160, Shimadzu, Kyto, Japan) using a proper Beer's plot. The drug contents in the samples were between 96.5% and 102.9% of the expected values.

Dissolution studies

The dissolution of chlorpropamide in powder form, physical mixture, and SDs was investigated using the Levy's beaker and stirrer method (Levy, 1961). A sample equivalent to 20 mg of the drug was added to 1000 mL

TABLE 1 **Dissolution Parameters of the Proposed Model for Different Formulations of Chlorpropamide in 0.1 M HCl (pH 1.1) and Phosphate Buffer (pH 7.25) Dissolution Media**

Set number	Formulation	Code	pH	m	b	$^{b}t_{50\%}$ (min)
1	Pure powder of chlorpropamide	PPA[c]	1.1	937.125	1.556	81.3
2	Physical mixture chlopropamide PH102 (1:5)[a]	PMA	1.1	55.534	1.080	41.2
3	SD chlopropamide Avicel PH102 (1:1)	SD1A	1.1	121.115	1.206	53.4
4	SD chlopropamide Avicel PH102 (1:2)	SD2A	1.1	183.874	1.936	14.8
5	SD chlopropamide Avicel PH102 (1:5)	SD5A	1.1	5.173	1.172	4.1
6	SD chlopropamide Avicel RC591 (1:1)	SDR1A	1.1	138.625	1.544	24.4
7	SD chlopropamide Avicel RC591 (1:2)	SDR2A	1.1	90.628	1.678	14.2
8	SD chlopropamide Avicel RC591 (1:5)	SDR5A	1.1	19.325	1.687	5.8
9	Pure powder of chlorpropamide	PPB[d]	7.25	2.893	0.581	6.2
10	SD chlopropamide Avicel PH102 (1:2)	SD2B	7.25	1.429	0.896	1.5
11	SD chlopropamide Avicel PH102 (1:5)	SD5B	7.25	0.136	1.517	0.3

[a]The figures inside the parentheses represents the ratio of drug to carrier. [b]According to the model the predicted time required for 50% dissolution is calculated by $t_{50\%}=m^{(1/b)}$. [c]Dissolution medium is 0.1 M HCl (pH 1.1) and [d]dissolution medium is phosphate buffer (pH 7.25).

of dissolution medium (either 0.1 M hydrochloric acid solution pH 1.1 or phosphate buffer solution pH 7.25). Table 1 shows the composition of each formulation as well as the medium used for its dissolution study. The mixture was stirred at 80 rpm with a two bladed stirrer 7.5 cm in diameter positioned 4 cm from the bottom of beaker, at 37 ± 0.3°C. Five milliliter samples of dissolution mixture were withdrawn at different time intervals, filtered and assayed at 232.6 nm for the acidic medium on the spectrophotometer. In the case of the phosphate medium the samples were acidified with 1 M HCl before the assay. The drug concentration in each sample was corrected considering the concentrations in the previous samples. Each dissolution test was carried out at least three times.

X-ray crystallography and IR spectroscopy

An automated powder diffractometer (Siemens-80, Munich, Germany) was employed to obtain X-ray diffraction patterns of the samples using Cu Kα radiation at a scan rate of 2° min^{-1} in terms of 2θ angle. The KBr disk sample preparation technique was used to prepare the IR spectra of the formulations on an IR spectrophotometer (FT-IR 3400, Shimadzu, Kyoto, Japan).

RESULTS AND DISCUSSION

The dissolution profiles of the drug powder, its physical mixture with Avicel PH-102 in the ratio of 1:5 and different SDs are given in Fig. 1. In order to obtain a meaningful kinetic parameter, the data presented in the figure was fitted to a novel model (see appendix for its theoretical justification) and the goodness of fit was compared with the different available dissolution models (Wagner, 1969; Costa & Sousa Lobo, 2001) including power law, first order, Weibull, cube root, square root, two-thirds power, linear probability and log-probability models. The proposed novel model denoted as reciprocal powered time model is as follows:

$$\left(\frac{1}{F_d}-1\right)=\frac{m}{t^b} \qquad (1)$$

where F_d is fraction of drug dissolved up to time t, b is a model parameter describing the shape of the dissolution

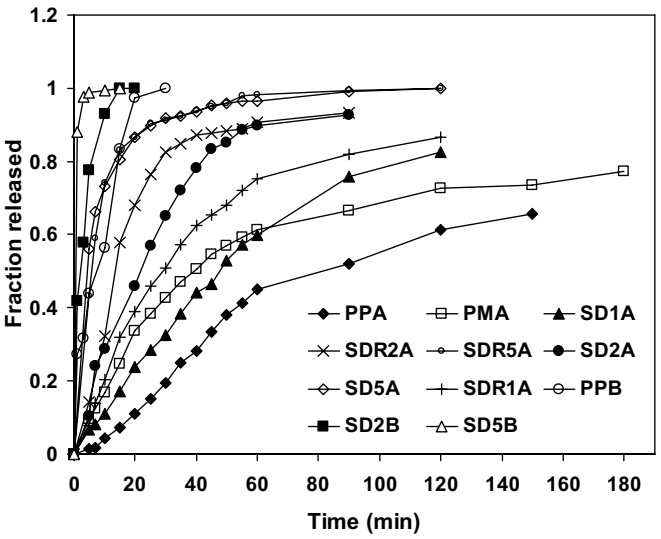

FIGURE 1 **The Dissolution Curves of Pure Chlorpropamide, its Physical Mixture With Microcrystalline Cellulose (1:5) and Various SD Formulations. Each Data Point is the Average of Three Values. For the Meanings of the Codes see Table 1.**

curve and m is another parameter of the model related to the time required for 50% dissolution, $t_{50\%}$, which in turn inversely related to the dissolution rate. The value of $t_{50\%}$ is in fact a kinetic parameter derived from the model. If in Eq. (1) F_d=0.5, t would be $t_{0.5}$ or $t_{50\%}$ and m equals $t_{0.5}^b$. Thus $t_{0.5}$ is calculated by Eq. (2).

$$t_{50\%}=m^{(1/b)} \qquad (2)$$

Eq. (1) can be used in either log-linear or nonlinear forms. The model parameters (m and b) in the latter form were obtained via a nonlinear iteration technique. Eq. (1) is valid for any F_d values greater than zero and less than unity and requires more than four data points to produce an accurate result. Calculations indicated that the accuracy of the nonlinear form was greater than that of the log-linear form and only the results of the nonlinear approach are given in Table 1 for different formulations. The values of $t_{50\%}$ for chlorpropamide pure powder and its 1:5 physical mixture with microcrystalline cellulose (Avicel PH-102) at pH 1.1 are 81.3 and 41.2 min, respectively, indicating a considerable increase of drug dissolution from the physical mixture. This is probably because of the adsorption of hydrophilic colloidal particles of microcrystalline cellulose onto the hydrophobic chlorpropamide particles which in turn enhances the wettability and the deaggregation of the latter particles (Leuner & Dressman, 2000; Barzegar-Jalali et al., 2002; Dastmalchi et al., 2005). It

can be seen from Fig. 1 and Table 1 that the drug dissolution rate depends on the type and amount of the carrier as well as the pH of the dissolution medium. In a given dissolution medium, the increase in the amount of both types of the carriers in the SDs resulted in enhanced dissolution rate. For example an increase in the amount of Avicel PH-102 from one part to five parts in the SD leads to a considerable increase in the dissolution rate as it is evident from thirteen fold decrease in the corresponding $t_{50\%}$ values (Table 1). The grade of the carrier also affected the dissolution rate. The dissolution of the drug from the SDs with the ratios of drug to carrier 1:1 and 1:2 containing Avicel RC-591 is greater than that from the SDs prepared of Avicel PH-102 with the same ratios (Table 1). This is because the former grade contains 10% (w/w) water soluble sodium carboxymethyl cellulose which improves the hydrophilicity of the carrier in comparison to the latter carrier. A slightly opposite effect was seen in the SDs with the ratio of 1:5 ($t_{50\%}$ values of 5.8 and 4.1 min for SDR5A and SD5A, respectively). This is probably because of the increased microenvironmental viscosity brought about by the higher concentration of sodium carboxymethyle cellulose around the chlorpropamide particles which might slow down diffusion of the drug molecules into dissolution medium.

Since chlorpropamide is a weakly acidic drug (pKa 5.0) its dissolution rate is substantially higher at pH 7.25 as compared with that of pH 1.1 (Fig. 1 and Table 1). This is in line with a previous finding (Taylor et al., 1977).

The higher the ratio of both carriers to drug (number of parts of carriers per unit part of drug) in the SDs the higher is the drug dissolution in both dissolution media. A quantitative relationship between reciprocal dissolution half-life ($1/t_{50\%}$) calculated from the reciprocal powered time model and carrier to drug ratio (CD) was established which could be of predictive value in practice. The relationships for different situations and the corresponding plots are seen in Fig. 2.

X-ray diffraction pattern of chlorpropamide obtained after evaporation of its solution in Cl_2CH_2 showed that the drug must have been converted to slightly reduced crystalline state as it was evident from low intensity of the peaks compared to that of the untreated drug powder. From characteristic peaks shown by asterisks in the diffractograms (Fig. 3), two peaks on the right hand side had the count values of 190 and 180 for the untreated drug powder. The count values for the corresponding peaks for the treated powder

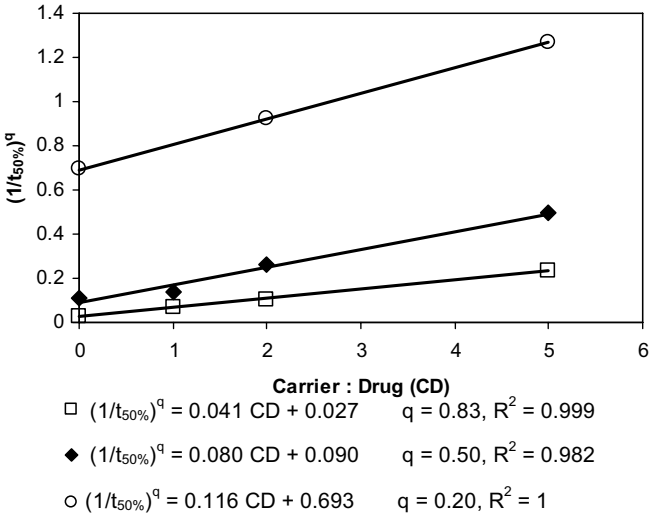

FIGURE 2 **Relationships Between Dissolution Half-life and Carrier to Drug Ratio (Parts of Carrier per Unit Part of Drug) for Pure Chlorpropamide Powder as well as its SDs Containing Avicel PH-102 in Phosphate Buffer Medium (○), Avicel PH-102 in Acidic Medium (◆) and Avicel RC-591 in Acidic Medium (□). The Relevant Equations are Given Above.**

were 155 and 170. On the other hand the IR spectra were identical indicating no drug interactions with solvent. In other words no crystal solvation or pseudopolymorphism was detected (Fig. 3). The IR spectra of SDs, e.g., SD (1:5) and its corresponding physical mixture, were also identical which meant no solvated crystal and/or pseudopolymorphism has occurred. But some appreciable reduced drug crystallinity was evident from the X-ray diffraction pattern of the SDs, as represented by smaller peaks (Fig. 4). For example the count values for the first three peaks from right hand side indicated by asterisks were 55, 80, and 110 for the physical mixture and 40, 55, and 80 for the corresponding SD formulation, respectively. From these findings, it is concluded that the enhanced drug dissolution for SDs is caused by the reduced crystallinity, the probable increase in effective surface area of the chlorpropamide as a result of the reduction of its particle size as well as its reduced tendency for aggregation and augmentation of its wettability by the carriers in the dissolution media (Fredrich et al., 2005).

The accuracy and prediction ability of the proposed model were compared with those of the commonly used models employing the following criteria:

$$MPD = \frac{100\sum_{i=1}^{n}\left[\left|F_{cal,i} - F_{obs,i}/F_{obs,i}\right|\right]}{n} \qquad (3)$$

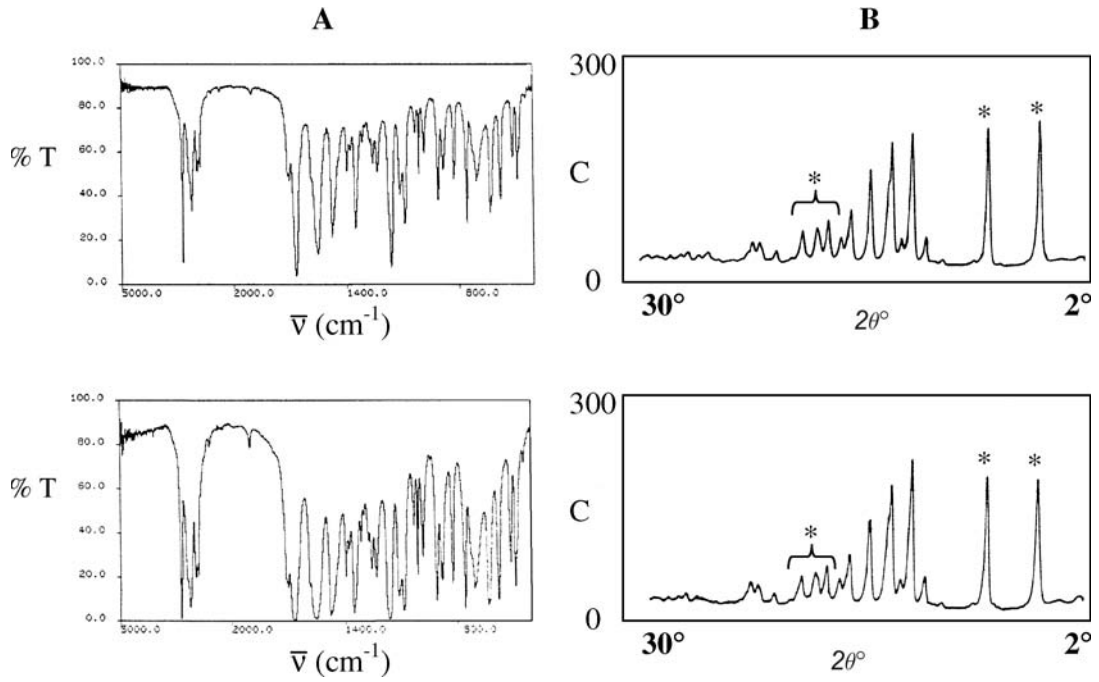

FIGURE 3 **Infrared Spectra (Panel A) and X-ray Diffraction Pattern (Panel B) of the Pure Chlorpropamide (Top) and Chlorpropamide Obtained Following Evaporation of its Solution in Methylene Chloride (Bottom). %T, ν, C and θ are Percent Transmittance, Wave Number, Counts and the Incidence Angle, Respectively. The Asterisks Show the Corresponding Peaks Changed Upon the Evaporation.**

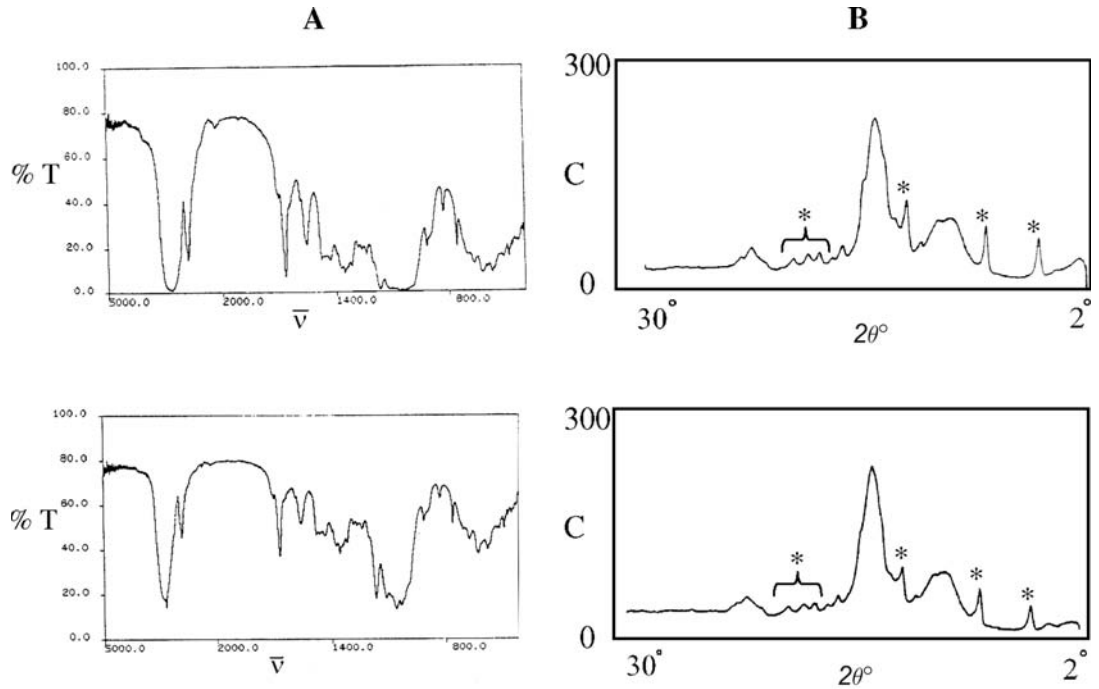

FIGURE 4 **Infrared Spectra (Panel A) and X-ray Diffraction Pattern (Panel B) of Physical Mixture of Chlopropamide:Avicel PH102 (1:5) (Top) and SD of Chlopropamide:Avicel PH102 (1:5) (Bottom). %T, ν, C and θ are Percent Transmittance, Wave Number, Counts and the Incidence Angle, Respectively. The Asterisks Show the Corresponding Peaks Changed Upon the Evaporation.**

$$OMPD = \frac{\sum_{i=1}^{11} (MPD)_i}{11} \qquad (4)$$

MPD is mean absolute percent deviation, n is the number of data in each set, $F_{\text{cal},\,i}$ and $F_{\text{obs},\,i}$, denote calculated fraction and observed fraction of drug dissolved at the i^{th} sample, respectively. *OMPD* is the

TABLE 2 **Mean Percent Deviation (MPD) and Overall Mean Percent Deviation (OMPD) of Various Models Together With Percent Number of Smaller MPDs of the Proposed Model (Reciprocal Powered Time) in Comparison With Other Models (PNSM)**

		MPDs of models								
Set number	Formulation	Reciprocal powered time	[a]Power law	[b]First order	[c]Weibull	[d]Cube root	[e]Square root	[f]Two-thirds power	[g]Probability	[h]Log-probability
1	PPA	10.85	23.58	45.33	13.83	59.21	64.83	69.76	71.12	8.11
		(0.987)	(0.953)	(0.961)	(0.973)	(0.943)	(0.932)	(0.921)	(0.762)	(0.992)
2	PMA	4.05	16.49	31.98	9.80	34.00	34.87	35.69	35.07	5.10
		(0.998)	(0.919)	(0.878)	(0.961)	(0.833)	(0.809)	(0.885)	(0.700)	(0.987)
3	SD1A	6.86	7.35	5.35	3.54	10.07	14.12	17.61	24.29	9.67
		(0.995)	(0.987)	(0.995)	(0.997)	(0.985)	(0.975)	(0.963)	(0.898)	(0.977)
4	SD2A	14.29	18.70	14.05	6.30	20.31	22.68	25.86	20.51	5.83
		(0.967)	(0.825)	(0.948)	(0.977)	(0.911)	(0.888)	(0.862)	(0.855)	(0.982)
5	SD5A	0.81	7.50	3.33	0.88	4.92	5.47	6.34	5.56	0.77
		(0.995)	(0.814)	(0.972)	(0.994)	(0.884)	(0.825)	(0.766)	(0.904)	(0.987)
6	SDR1A	7.80	13.57	24.10	6.70	29.79	31.91	33.85	32.15	2.04
		(0.995)	(0.929)	(0.951)	(0.977)	(0.905)	(0.878)	(0.850)	(0.789)	(0.998)
7	SDR2A	3.73	3.88	27.14	9.88	28.55	29.03	31.27	26.88	6.65
		(0.998)	(0.909)	(0.845)	(0.921)	(0.765)	(0.722)	(0.683)	(0.695)	(0.964)
8	SDR5A	1.78	15.29	5.75	2.95	7.75	8.47	9.78	7.34	2.03
		(0.995)	(0.927)	(0.970)	(0.971)	(0.864)	(0.789)	(0.712)	(0.881)	(0.975)
9	PPB	16.03	12.45	30.53	18.57	13.26	8.97	6.91	7.39	25.10
		(0.844)	(0.924)	(0.876)	(0.831)	(0.944)	(0.966)	(0.980)	(0.969)	(0.755)
10	SD2B	7.63	3.82	26.98	9.39	2.58	4.20	7.99	2.64	16.39
		(0.948)	(0.980)	(0.895)	(0.906)	(0.992)	(0.987)	(0.959)	(0.976)	(0.814)
11	SD5B	0.16	1.94	2.24	0.90	2.43	2.56	2.70	2.32	0.79
		(0.998)	(0.831)	(0.764)	(0.937)	(0.669)	(0.626)	(0.588)	(0.716)	(0.954)
OMPD	—	6.73	11.32	19.71	7.52	19.35	20.65	22.52	21.30	7.50
PNSM	—	—	72.73	81.82	72.73	81.82	81.82	90.91	81.82	63.60

The figures inside parentheses are the values of R^2 of the models. [a]In linear form: $\mathrm{Ln}F=\mathrm{Ln}k_p + p\mathrm{Ln}t$; [b]$\mathrm{Ln}(1-F)=-\mathrm{Ln}k_f.t$; [c]$\mathrm{Ln}[-\mathrm{Ln}(1-F)]=\mathrm{Ln}k_w + a\mathrm{Ln}t$; [d]$1-(1-F)^{1/3}=k_{1/3}.t$; [e]$1-(1-F)^{1/2}=k_{1/2}.t$; [f]$1-(1-F)^{2/3}=k_{2/3}.t$; [g]$Z=Z_0 + Mt$; [h]$Z=Z_0 + M'\mathrm{Ln}t$. F denotes fraction of drug dissolved up to time t, k_p, p, k_f, k_w, a, $k_{1/3}$, $k_{1/2}$, $k_{2/3}$, Z_0, M and M' are parameters of the models. Z is probit of percent drug dissolved at any time.

overall mean percent deviation. In addition to these criteria a third criterion namely the number of smaller *MPDs* associated with the proposed model in comparison with the other models expressed as the percentage (PNSM) also was employed. The smaller the value of *MPD* for a given model and particular set of data indicates that the model predicts the fraction of drug dissolved closer to the experimental fractional drug dissolution. In the same manner, the smaller *OMPD* which is the average of *MPD*s of all of the eleven data sets obtained for a given model implies the accuracy of the model. For example the *MPD* values of the reciprocal powered time and first order models for pure drug powder (PPD in Table 2) are 10.85 and 45.33 percentages respectively. Also the corresponding *OMPD* values of the same models for eleven data sets are 6.73 and 19.71. Considering the *OMPD* values the accuracy of the models in descending order are: Reciprocal powered time > log-probability > Weibull > power law > cube root > first order > square root > probability > two thirds power. The value of PNSM higher than 50% indicates that the proposed model is superior from this respect to the other models. The higher the PNSM value from 50% the more accurate is the proposed model relative to the model under consideration. From this stand point the accuracy of the classic models after the reciprocal powered time model in descending order are: log-probability > power law=Weibull > first order=cube root=square root=probability models > two-thirds power models. The analysis given above reveals that the proposed model is superior to six commonly used models with the exception of log-probability and Weibull models from *OMPD* point of view. The corresponding values of *OMPD* for the proposed and the latter two models are 6.73, 7.50, and 7.52, respectively. But the superiority of the model is evident from its higher percentage of the number of smaller *MPD*s, i.e., PNSM as compared to the two mentioned models with the PNSM values of 63.60 and 72.73, which means the model in seven and eight sets out of eleven sets produces smaller *MPD*s in comparison to log-probability and Weibull models, respectively.

CONCLUSION

The dissolution rate of the water insoluble drug chlorpropamide can be enhanced via solvent deposition technique by the use of two grades of water insoluble but highly hydrophilic microcrystalline cellulose carriers. The carrier with higher hydrophilicity produced faster dissolution. The higher the ratio of the carrier to drug the greater is the dissolution rate and a quantitative correlation exists between the ratio and the dissolution half-life. At higher pH the dissolution rate of the drug from preparations is higher. X-ray diffraction showed some reduced drug crystallinity in SDs, while IR spectroscopy revealed no interactions between the drug and solvent as well as the carriers. The observed differences in the dissolution rates are because of the reduced drug crystallinity, probable decreased particle size, increased wettability and reduced aggregation of the hydrophobic drug particles. Also the reciprocal powered time model proposed in this study is an accurate kinetic model for analyses of the dissolution data as compared with commonly used models.

ACKNOWLEDGMENT

The authors would like to thank the Vice-chancellery for Research of Tabriz University of Medical Sciences for the financial support.

REFERENCES

Barzegar-Jalali, M., Maleki, N., Garjani, A., Khandar, A. A., Haji-Hosseinloo, M., Jabbari, R., & Dastmalchi, S. (2002). Enhancement of dissolution rate and anti-inflammatory effects of piroxicam using solvent deposition technique. *Drug Development and Industrial Pharmacy, 28*, 681–686.

Batenhorst, R. L., Bustrack, J. A., Bivins, B. A., & Foster, T. S. (1982). Comparative bioavailability of chlorpropamide tablet and suspension formulations. *Clinical Pharmacy, 1*, 58–61.

Costa, P., & Sousa Lobo, J. M. (2001). Modeling and comparison of dissolution profiles. *European Journal of Pharmaceutical Sciences, 13*, 123–133.

Dastmalchi, S., Garjani, A., Maleki, N., Sheikhee, G., Baghchevan, V., Jafari-Azad, P., Valizadeh, H., & Barzegar-Jalali, M. (2005). Enhancing dissolution, serum concentrations and hypoglycemic effect of glibenclamide using solvent deposition technique. *Journal of Pharmacy and Pharmaceutical Sciences, 8*, 175–181.

Deshpande, A. V., & Agrawal, D. K. (1983). Increasing the dissolution rate of chlorpropamide by dispersion technique using various dispersing agents. *Pharmazie, 38*, 539–541.

Deshpande, A. V., & Agrawal, D. K. (1984). Effect of different grades of polyvinylpyrrolidone on dissolution rate of chlorpropamide and its absorption through rat stomach. *Drug Development and Industrial Pharmacy, 10*, 1725–1736.

Deshpande, A. V., & Agrawal, D. K. (1985). Bioavailability studies of chlorpropamide from its polyvinylpyrrolidone coprecipitate. *Pharmazie, 40*, 496–497.

Dubois, J. L., & Ford, J. L. (1985). Similarities in the release rates of different drugs from polyethylene glycol 6000 solid dispersions. *Journal of Pharmacy and Pharmacology, 37*, 494–495.

Evans, M., Glass, R. C., Mitchard, M., Munday, B. M., & Yates, R. (1979). Bioavailability of chlorpropamide. *British Journal of Clinical Pharmacology, 7*, 101–105.

Ford, J. L., & Rubinstein, M. H. (1977). The effect of composition and ageing on the dissolution rates of chlorpropamide-urea solid dispersions. *29*, 688–694.
Fredrich, H., Nada, A., & Bodmeier, R. (2005). Solid state and dissolution rate characterization of co-graound mixtures of nifedipine and hydrophilic carriers. *Drug Development and Industrial Pharmacy, 31*, 719–728.
Leuner, C., & Dressman, J. (2000). Improving drug solubility for oral delivery using solid dispersions. *European Journal of Pharmaceutics and Biopharmaceutics, 50*, 47–60.
Levy, G. (1961). Comparison of dissolution and absorption rates of different commercial aspirin tablets. *Journal of Pharmaceutical Sciences, 50*, 388–392.
Noyes, A. A., & Whitney, W. R. (1897). The rates of solution of solid substances in their own solutions. *Journal American Chemical Society, 19*, 930–934.
Sweetman, S. C. (2005) Martindale: The complete drug reference. Pharmaceutical Press, London.
Taylor, T., Assinder, D. F., Chasseaud, L. F., Bradford, P. M., & Burton, J. S. (1977). Plasma concentrations, bioavailability and dissolution of chlorpropamide. *European Journal of Clinical Pharmacology, 11*, 207–212.
Van Der Watt, J. G., Parrott, E. L., & Devilliers, M. M. (1996). A comparison of interaction and solvent deposition mixing. *Drug Development and Industrial Pharmacy, 22*, 741–746.
Wagner, J. G. (1969). Interpretation of percent dissolved-time plots derived from in vitro testing of conventional tablets and capsules. *Journal of Pharmaceutical Sciences, 58*, 1253–1257.
Yen, S. Y., Chen, C. R., Lee, M. T., & Chen, L. C. (1997). Investigation of dissolution enhancement of nifedipine by deposition on superdisintegrants. *Drug Development and Industrial Pharmacy, 23*, 313–317.

APPENDIX

According to the Noyes-Whitney law (Noyes & Whitney, 1897) the dissolution rate, dW/dt, under the sink conditions is given by:

$$dW/dt = kC_sS \tag{A1}$$

in which k, C_s and S are the dissolution rate constant, solubility of solid drug in dissolution medium and the effective surface area of the solid at any time, respectively. The integration of Eq. (A1) between time zero and t as well as infinity, ∞, results in:

$$W = kC_s\int_0^t Sdt \tag{A2}$$

$$W_\infty = kC_s\int_0^\infty Sdt \tag{A3}$$

W and W_∞ denote the amounts of solid dissolved up to times t and ∞. The integrals $\int_0^t Sdt$ and $\int_0^\infty Sdt$ are cumultive surface areas exposed for dissolution from times 0 to t and 0 to ∞. Subtraction of Eq. (A2) from Eq. (A3) yields:

$$W_\infty - W = M = kC_s\left[\int_0^\infty Sdt - \int_0^t Sdt\right] = kC_s\int_t^\infty Sdt \tag{A4}$$

where M is amount of undissolved solid at time t, and $\int_t^\infty Sdt$ is cumulative surface area remaining to be exposed for dissolution from time t to ∞.

The fraction of the drug dissolved, F_d, is given by:

$$F_d = \frac{W}{W_\infty} = \frac{W}{W+M} = \frac{kC_s\int_0^t Sdt}{kC_s\int_0^t Sdt + kC_s\int_t^\infty Sdt} = \frac{\int_0^t Sdt}{\int_0^t Sdt + \int_t^\infty Sdt} \tag{A5}$$

The term on the far right hand side of Eq. (A5) in fact equals fraction of cumulative surface area exposed for dissolution up to time t, F_S. Therefore, the fraction of the drug dissolved equals F_S. Since $\int_0^t Sdt$ increases with time and the opposite is true for $\int_t^\infty Sdt$, it is assumed that the power equations in the forms of $\int_0^t Sdt = \alpha \cdot t^a$ and $\int_t^\infty Sdt = \beta \cdot t^{-a'}$ hold for the cumulative surface areas in which α, β, a and a' are constants. Thus substitution of the corresponding values of the integrals from the power equations into Eq. (A5) yields:

$$F_d = \frac{\alpha \cdot t^a}{\alpha \cdot t^a + \beta \cdot t^{-a'}} = \frac{\alpha \cdot t^{a+a'}}{\alpha \cdot t^{a+a'} + \beta} = \frac{t^b}{t^b + (\beta/\alpha)} = \frac{t^b}{t^b + m} \tag{A6}$$

where b is the shape factor and equals $a + a'$. Also m equals β/α. Eq. (1) in the text can be readily obtained from reciprocating Eq. (A6) and subsequent rearrangement.